Acta Crystallographica Section B
**Structural Science**
ISSN 0108-7681

# Structure of $LaTi_2Al_9O_{19}$ and reanalysis of the crystal structure of $La_3Ti_5Al_{15}O_{37}$

**Marta Kasunič,[a] Anton Meden,[a] Srečo D. Škapin,[b] Danilo Suvorov[b] and Amalija Golobič[a]***

[a]Faculty of Chemistry and Chemical Technology, University of Ljubljana, Aškerčeva 5, Ljubljana 1000, Slovenia, and [b]Jožef Stefan Institute, Jamova 39, Ljubljana 1000, Slovenia

Correspondence e-mail: amalija.golobic@fkkt.uni-lj.si

Received 23 September 2011
Accepted 27 September 2011

The non-perovskite compound $LaTi_2Al_9O_{19}$ was synthesized and structurally characterized by conventional X-ray powder diffraction and shown to be isostructural with $SrTi_3Al_8O_{19}$, as confirmed by bond-valence sum calculations. The dielectric properties of $LaTi_2Al_9O_{19}$ at 1 MHz were measured. The crystal structure of $La_3Ti_5Al_{15}O_{37}$, which is referred to as the most complex structure solved *ab initio* from X-ray powder diffraction (XRPD) to date, is shown to be incorrect.

## 1. Introduction

In order to stabilize $La_{2/3}TiO_3$ and consequently to prepare new compounds with promising microwave and dielectric properties applicable in electronics, the ternary system $La_2O_3$–$TiO_2$–$Al_2O_3$ has been studied extensively (Škapin *et al.*, 1993; Suvorov *et al.*, 1998). The crystal structures of several ternary oxides have been determined:

(i) *A*-site deficient perovskites including $La_{0.68}Al_{0.05}Ti_{0.95}O_3$ (Ali *et al.*, 2006), $La_{0.7}Al_{0.1}Ti_{0.9}O_3$ and $La_{0.717}Al_{0.15}Ti_{0.85}O_3$ (Yoshioka, 1994);

(ii) a perovskite with vacancies distributed among all sites, $La_{0.9}Al_{0.465}Ti_{0.465}O_{2.9}$ (Slater & Irvine, 1999);

(iii) $La_5AlTi_3O_{15}$ (Kuang *et al.*, 2006) as an example of a *B*-deficient hexagonal perovskite.

The only non-perovskite structure known is $La_3Ti_5Al_{15}O_{37}$ and with 60 atoms in the asymmetric unit it is one of the largest structures determined from powder diffraction data and solved by *ab initio* methods (Morris *et al.*, 1994).

Here we report the crystal structure and dielectric properties of another non-perovskite in the $La_2O_3$–$TiO_2$–$Al_2O_3$ system with the formula $LaTi_2Al_9O_{19}$, whose synthesis and unit-cell parameters were described by Morgan (1984). The X-ray powder diffraction pattern of $LaTi_2Al_9O_{19}$ is in the PDF-2 database (PDF card No. 000-037-1233), but after the structural characterization of $La_3Ti_5Al_{15}O_{37}$ (Morris *et al.*, 1994) PDF card 37-1233 was misnamed as $La_3Ti_5Al_{15}O_{37}$ owing to the similarity of powder patterns and preparation procedures (*PDF*-2; ICDD, 2009*a*,*b*). In the latest database $LaTi_2Al_9O_{19}$ was restored. The aim of this study is to remove the ambiguity surrounding the composition and structure of these non-perovskite lanthanum aluminotitanates.

## 2. Experimental

Single-phase $LaTi_2Al_9O_{19}$ ceramic was prepared according to Morgan (1984) by mixing high-purity $La_2O_3$ (Alfa Aesar, 99.99%) with Ti isopropoxide (Sigma-Aldrich, 97%) in 2-propanol, followed by the addition of an aqueous solution of $Al(NO_3)_3$ (Johnson Matthey) in an agate mortar. The dried

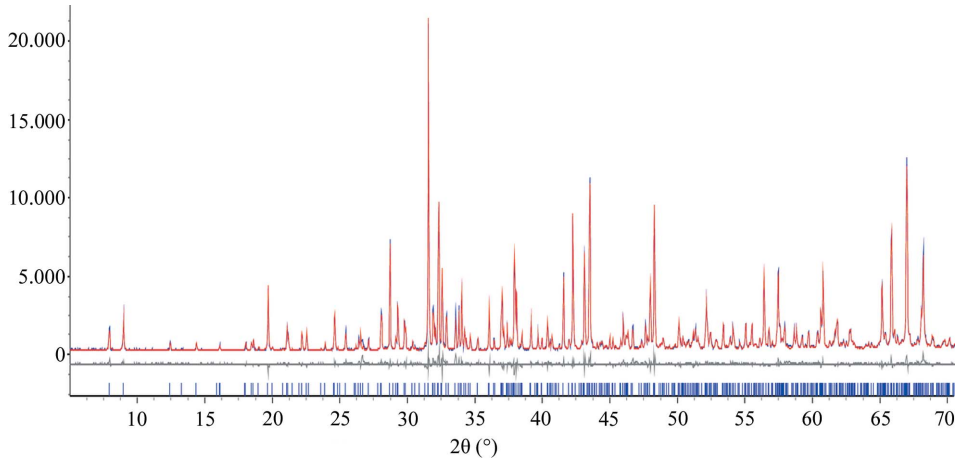


**Figure 1**
Rietveld plot for $LaTi_2Al_9O_{19}$ (experimental = blue, calculated = red, difference profile = grey). Lower vertical bars represent reflection positions. This figure is in colour in the electronic version of this paper.

**Table 1**
Experimental details.

| | |
|---|---|
| Crystal data | |
| Chemical formula | $Al_9LaO_{19}Ti_2$ |
| $M_r$ | 781.47 |
| Crystal system, space group | Monoclinic, *C*2/*c* |
| Temperature (K) | 293 |
| *a*, *b*, *c* (Å) | 22.59355 (18), 10.99919 (9), 9.72968 (7) |
| $\beta$ (°) | 98.5634 (5) |
| *V* (Å$^3$) | 2390.97 (3) |
| *Z* | 8 |
| Radiation type | Cu $K\alpha_1$, $\lambda$ = 1.54059 Å |
| $\mu$ (mm$^{-1}$) | 46.126 |
| Specimen shape and colour | Irregular pale yellow powder |
| Data collection | |
| Diffractometer | PANalytical X'Pert PRO MPD |
| Specimen mounting | Flat plate |
| Data collection mode | Reflection |
| Scan method | Step |
| $2\theta$ values (°) | $2\theta_{min}$ = 5, $2\theta_{max}$ = 120, $2\theta_{step}$ = 0.033 |
| Refinement | |
| *R* factors and goodness of fit | $R_p$ = 0.049, $R_{wp}$ = 0.067, $R_{exp}$ = 0.034, $R_{Bragg}$ = 0.031, $\chi^2$ = 4.004 |
| No. of data points | 3485 |
| No. of parameters | 109 |
| No. of restraints | 0 |

Computer programs: *TOPAS-Academic* (Coelho, 2007), *ATOMS* (Dowty, 2005).

mixture was uniaxially pelletized at ~ 100 MPa and fired with a heating rate of 5 K min$^{-1}$ to 873 K. Subsequently, the sintering temperature was increased to 1723 K (1 K min$^{-1}$) and held for 10 h before cooling to ambient temperature in the furnace. For electrical measurements thin tablets were cut from the pellet. Silver paste was applied to both sides of the tablets and bonded at 823 K. The capacitance and dielectric losses were measured at 1 MHz using an Agilent 4284A LCR meter from 293 to 363 K. Polished and thermally etched cross sections were analyzed by using a field-emission scanning electron microscope (FESEM; SUPRA 35VP Carl Zeiss), equipped with an energy-dispersive spectrometer (EDXS; Inca 400, Oxford Instruments). X-ray powder diffraction data were collected using a PANalytical X'Pert PRO MPD diffractometer with $\theta$–$2\theta$ reflection geometry and primary side Johansson type monochromator. The crystal data, collection conditions and refinement parameters are presented in Table 1.

The starting model for Rietveld refinement used the unit-cell parameters and atomic coordinates of isostructural *C*2/*c* $SrAl_8Ti_3O_{19}$ (Strunk & Mueller-Buschbaum, 1993) with lanthanum entering the strontium site and two titanium replaced by aluminium. The first Ti/Al replacement was made at the only 8*f* site in the Sr compound which was statistically occupied by both species, *i.e.* Al9 and Ti4. The second titanium site replaced by aluminium is Ti3 which is reasonable from two points of view. First, this is the only atom that occupies the special position (4*e*) and consequently partial occupancy and/or disorder is not required to obtain agreement with the nominal composition. Second, within 4 Å of this site there is the largest number of $Sr^{2+}$ ions that when replaced by $La^{3+}$ can be effectively charge-balanced by lower valent $Al^{3+}$. Several other substitutions to change the Al:Ti ratio from 8:3 to 9:2 were tested, but resulted in significantly poorer fits between the calculated and observed powder patterns and non-physical bond-valence sums.

Rietveld refinement was performed using the *TOPAS-Academic* program suite (Coelho, 2007). In the first refinement cycles the background was modelled by a third-order polynomial, while the zero error and scale factor were also refined. In the next steps, the cell parameters, atomic coordinates and a global isotropic displacement parameter were released. The Bragg reflections were modelled using a Thompson–Cox–Hastings pseudo-Voigt function (Thompson *et al.*, 1987). Altogether, 109 independent parameters were refined. The final match between observed and calculated profiles between 5–70° $2\theta$ is shown in Fig. 1, and Rietveld plots between 5–120 and 70–120° $2\theta$ have been deposited.[1]

## 3. Results and discussion

### 3.1. Crystal structure of $LaTi_2Al_9O_{19}$

The fundamental units of the title compound are $AlO_6$ and $TiO_6$ octahedra which are connected through lanthanum ions and $AlO_4$ tetrahedra as in $SrAl_8Ti_3O_{19}$ (Strunk & Mueller-Buschbaum, 1993). The octahedral motif is quite complicated, and most obvious when viewed as (100) planes separated by

[1] Supplementary data for this paper are available from the IUCr electronic archives (Reference: HW5019). Services for accessing these data are described at the back of the journal.

around 3 Å. In the unit cell, ten layers stack along [100] (Fig. 2). The layers are of three types: layer *A* (at $x \simeq 0$ and $x \simeq 0.5$), layer *B* (at $x \simeq 0.1$, 0.4, 0.6 and 0.9) and layer *C* (at $x \simeq 0.2$, 0.3, 0.7 and 0.8; Figs. 3–5).

The type *A* layer contains $[Al_2O_{10}]$ pairs of edge-sharing octahedra. Four free vertices of the first octahedron from each pair are connected to four $AlO_4$ tetrahedra within the layer, and four free vertices of the second octahedron are shared with four lanthanum ions, either side of the layer (*i.e.* two from each of the neighbouring *B* layers).

Type *B* and *C* layers are very similar and contain the characteristic $(TiAl_5Ti)O_{28}$-serrated motif of edge-sharing octahedra. In layer *B* these components are connected to six similar groups within the same layer *via* two $AlO_6$ octahedra and six lanthanum ions. In layer *C* the connections are *via* six $AlO_4$ alone. The major difference between the layers is the presence of $La^{3+}$ ions in *B* layers and their absence in *C* layers

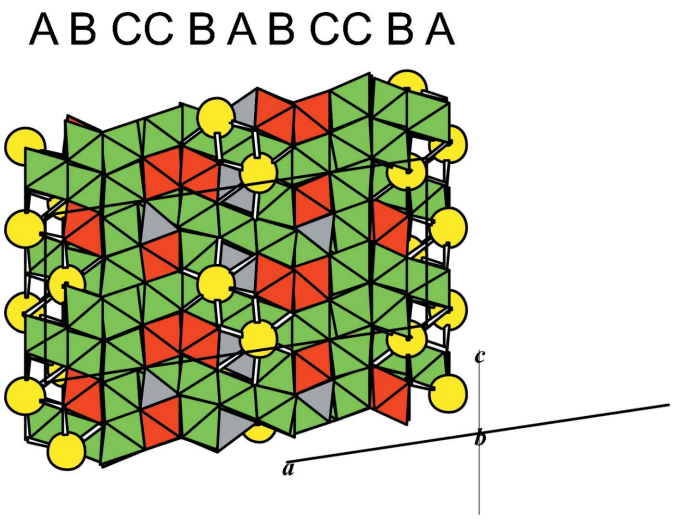


**Figure 2**
The stacking of octahedral layers in $LaTi_2Al_9O_{19}$ (green = $AlO_6$ octahedra, red = $TiO_6$ octahedra, grey = $AlO_4$ tetrahedra, yellow circles = $La^{3+}$ ions). This figure is in colour in the electronic version of this paper.

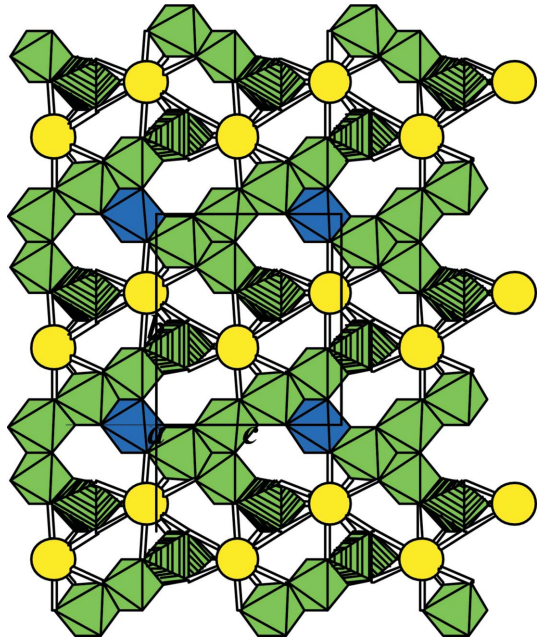


**Figure 4**
Representation of layer *B* at $x \simeq 0.1$ (green = $AlO_6$ octahedra, green hatched = $TiO_6$ octahedra, blue = $AlO_6$ octahedra that connect serrated units, yellow = $La^{3+}$ ions as described in text). This figure is in colour in the electronic version of this paper.

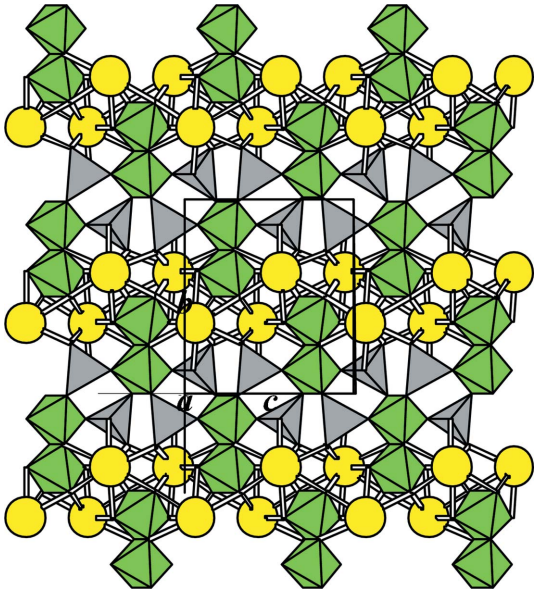


**Figure 3**
Representation of layer *A* at $x \simeq 0$ with $La^{3+}$ ions from neighbouring *B* layers (green = $AlO_6$ octahedra, grey = $AlO_4$ tetrahedra, yellow circles = $La^{3+}$ ions). This figure is in colour in the electronic version of this paper.

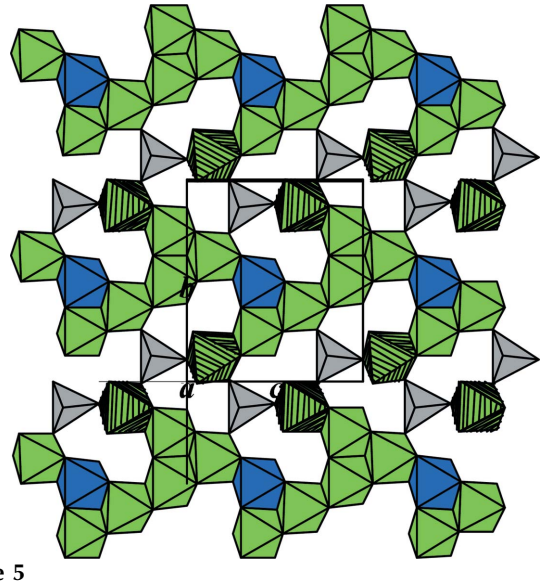


**Figure 5**
Representation of layer *C* at $x \simeq 0.2$ (green = $AlO_6$ octahedra, green hatched = $TiO_6$ octahedra, blue = $AlO_6$ octahedra that connect serrated units, grey = $AlO_4$ tetrahedra as described in text). This figure is in colour in the electronic version of this paper.

**Table 2**
Problematic structural segments in $La_3Ti_5Al_{15}O_{37}$ (CN = coordination number, $M$ = metal).

| Atom $A1$ | Atom $A2$ | Distance $A1-A2$ | CN of A1 |
|---|---|---|---|
| La1$^{i}$ | Al14$^{ii}$ | 3.08 (3) | 15 (12 O + 3 $M$) |
| | Ti2$^{i}$ | 3.15 (6) | |
| | Al10$^{iii}$ | 3.18 (5) | |
| Ti1$^{i}$ | Al4$^{i}$ | 2.27 (6) | 10 (6 O + 4 $M$) |
| | Al6$^{i}$ | 2.29 (6) | |
| | Al1$^{i}$ | 2.37 (6) | |
| | Al2$^{ii}$ | 2.46 (5) | |
| Ti4$^{i}$ | Al2$^{i}$ | 2.24 (10) | 7 (6 O + 1 $M$) |
| Ti5$^{i}$ | Al6$^{i}$ | 2.29 (10) | 8 (6 O + 2 $M$) |
| | Al1$^{i}$ | 2.48 (10) | |
| Al5$^{i}$ | Al4$^{i}$ | 2.37 (5) | 7 (6 O + 1 $M$) |
| Al13$^{i}$ | Al15$^{i}$ | 2.38 (7) | 7 (6 O + 1 $M$) |
| O3$^{i}$ | Ti1$^{i}$ | 1.67 (4) | 6 |
| | Ti4$^{ii}$ | 2.05 (9) | |
| | Ti5$^{i}$ | 1.89 (7) | |
| | Al1$^{i}$ | 1.86 (6) | |
| | Al2$^{ii}$ | 1.97 (5) | |
| | Al6$^{i}$ | 1.76 (6) | |

Symmetry codes: (i) $x, y, z$; (ii) $x+\frac{1}{2}, -y+\frac{3}{2}, z+\frac{1}{2}$; (iii) $x+\frac{1}{2}, -y+\frac{1}{2}, z+\frac{1}{2}$.

which only include $AlO_4$ tetrahedra. The sequence of layers is $\ldots BCCBABCCB\ldots$ (Fig. 2) linked by edge- and vertex-sharing octahedra between $A$–$B$ and $C-C$ layers, whereas the connections between the $B$ and $C$ layers is only through corner connection. Face-sharing octahedra are absent and $AlO_4$ tetrahedra connect with other fragments through vertices, leading to a 12-fold coordination of lanthanum.

### 3.2. Dielectric properties of $LaTi_2Al_9O_{19}$

The permittivity of $LaTi_2Al_9O_{19}$, measured at 1 MHz is slightly lower ($\epsilon$ = 17.4) than observed by Zhang & McGinn (2006) who found $\epsilon$ = 21 by near-field scanning microwave microscopy. A relatively low dielectric constant is expected owing to the significant proportion of aluminium, as higher permittivities require $MO_6$ octahedra, where the metal valence is 4 or higher (Herbert, 1985). However, the electric loss ($\tan\delta = 6\times10^{-4}$) is quite low and therefore promising for use in electronic components. The temperature coefficient ($\tau_k$) measured from 293 to 363 K is moderate ($\tau_k$ = 140 p.p.m. $K^{-1}$).

### 3.3. Reassessment of the $La_3Ti_5Al_{15}O_{37}$ crystal structure

In view of the foregoing analysis we have re-examined the *ab initio* structure solution reported as $La_3Ti_5Al_{15}O_{37}$ and found a number of inconsistencies (Morris *et al.*, 1994).

**3.3.1. Composition problem**. The present study, as well as the original synthesis (Morgan, 1984) and the later work of Morris *et al.* (1994) used the same synthesis procedure with the molar ratio La:Ti:Al = 1:2:9 that leads to a single-phase product with practically the same powder pattern. On that basis, Morgan (1984) formulated the product as $LaTi_2Al_9O_{19}$, confirmed here by elemental analysis. Additionally, secondary electron images/backscattered electron images (SEI/BSI) microscopy (Fig. 6) confirmed the phase purity. However, Morris *et al.* (1994) proposed the significantly different formula $La_3Ti_5Al_{15}O_{37}$, without supporting elemental analyses. Mass balance demands an aluminous impurity should be present; comparing the ratios La:Ti:Al 1:2:9 = 3:6:27 in the reaction mixture and 3:5:15 in the product. Morris *et al.* (1994) found the material used in laboratory X-ray and synchrotron data collection contained rutile while neutron diffraction data were impurity free.

**Table 3**
Bond-valence sums (BVS) for metal ions and metal–oxygen distance ranges for the title compound (CN = coordination number).

| Metal ion | CN | Distance ranges $M-O$ (Å) | BVS |
|---|---|---|---|
| La1 | 12 | 2.513 (21)–3.011 (17) | 2.660 |
| Ti1 | 6 | 1.84 (2)–2.174 (15) | 4.499 |
| Ti2 | 6 | 1.752 (22)–2.13 (2) | 4.222 |
| Al1 | 4 | 1.715 (17)–1.79 (3) | 2.711 |
| Al2 | 6 | 1.78 (3)–2.01 (3) | 2.679 |
| Al3 | 4 | 1.72 (2)–1.80 (2) | 2.648 |
| Al4 | 6 | 1.86 (3)–1.923 (15) | 2.870 |
| Al5 | 6 | 1.753 (21)–2.03 (3) | 3.190 |
| Al6 | 6 | 1.83 (3)–2.14 (3) | 2.624 |
| Al7 | 6 | 1.87 (3)–2.03 (3) | 2.450 |
| Al8 | 6 | 1.800 (18)–1.98 (3) | 2.665 |
| Al9 | 6 | 1.84 (3)–2.03 (3) | 2.577 |
| Al10 | 6 | 1.86 (3)–1.92 (3) | 2.843 |

**3.3.2. Structure problem**. Rietveld refinement of $La_3Ti_5Al_{15}O_{37}$ resulted in good agreement between calculated and observed diffraction patterns, but a detailed inspection of the crystal structure of $La_3Ti_5Al_{15}O_{37}$ reveals several problematic structural segments (Table 2). Specifically, some titanium and aluminium cations are separated by 2.2–2.5 Å which is unreasonable, leading to unusually large coordination numbers. Unreasonably short distances (< 3.2 Å) also appear between La and Ti or La and Al. In addition, the O3 atom is surrounded by six high-valence cations (three $Ti^{4+}$ and three $Al^{3+}$) 1.67–2.05 Å distant.

**3.3.3. Bond-valence sum calculations**. Bond-valence sums (BVS; Brown, 1992) for $LaTi_2Al_9O_{19}$ (Tables 3 and 4) are close to the nominal atomic valences (AV) (+3, +4, +3 and −2 for Al, Ti, La and O), which is reflected in a global instability

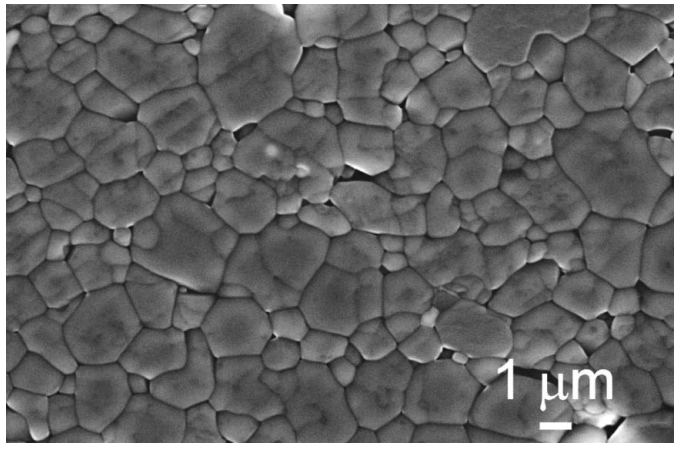


**Figure 6**
SEI/BSI micrographs of etched cross section of the ceramic based on the compound $LaTi_2Al_9O_{19}$, sintered at 1723 K for 20 h.

**Table 4**
Bond-valence sums (BVS) for oxygen ions and O—Ti/Al and O—La distance ranges for the title compound (CN = coordination number).

| Oxygen | CN | Distance ranges O—Ti/Al (Å) | Distance ranges O—La (Å) | BVS |
|---|---|---|---|---|
| O1 | 3 | 1.79 (3)–1.84 (3) | – | −1.803 |
| O2 | 4 | 1.72 (2)–1.91 (2) | 2.590 (22)–2.823 (20) | −2.018 |
| O3 | 5 | 1.91 (3)–1.92 (3) | 2.723 (21)–2.936 (20) | −1.774 |
| O4 | 4 | 1.918 (21)–1.979 (19) | – | −1.615 |
| O5 | 4 | 1.78 (3)–2.13 (2) | – | −1.876 |
| O6 | 4 | 1.781 (19)–2.03 (3) | – | −1.749 |
| O7 | 4 | 1.849 (14)–2.03 (3) | 2.562 (15) | −1.942 |
| O8 | 3 | 1.715 (17)–1.924 (17) | – | −2.015 |
| O9 | 4 | 1.84 (2)–1.92 (2) | 2.742 (21) | −2.051 |
| O10 | 3 | 1.752 (22)–1.905 (21) | – | −2.142 |
| O11 | 4 | 1.80 (2)–1.95 (3) | – | −1.925 |
| O12 | 4 | 1.793 (17)–1.99 (3) | 2.66 (3) | −1.740 |
| O13 | 4 | 1.79 (3)–2.04 (2) | – | −1.904 |
| O14 | 4 | 1.83 (3)–1.96 (2) | 2.513 (21) | −1.838 |
| O15 | 5 | 1.86 (3)–2.14 (3) | 2.950 (21) | −1.889 |
| O16 | 5 | 1.80 (3)–2.174 (15) | 2.87 (3)–3.011 (17) | −1.708 |
| O17 | 4 | 1.770 (15)–2.02 (3) | – | −1.876 |
| O18 | 3 | 1.78 (3)–1.967 (18) | – | −1.822 |
| O19 | 3 | 1.753 (21)–1.966 (22) | – | −2.095 |

**Table 5**
Bond-valence sums (BVS) and metal–oxygen distance ranges for $La_3Ti_5Al_{15}O_{37}$ (CN = coordination number).

| Metal ion | CN | Distance ranges $M$—O (Å) | BVS |
|---|---|---|---|
| La1 | 11 | 2.52 (3)–2.94 (4) | 2.346 |
| La2 | 12 | 2.23 (4)–3.00 (4) | 3.505 |
| La3 | 12 | 2.60 (4)–2.94 (4) | 2.404 |
| Ti1 | 6 | 1.61 (5)–2.36 (5) | 5.469 |
| Ti2 | 6 | 1.70 (7)–2.26 (7) | 4.254 |
| Ti3 | 6 | 1.68 (8)–2.25 (8) | 4.483 |
| Ti4 | 6 | 1.79 (9)–2.19 (9) | 4.392 |
| Ti5 | 6 | 1.70 (8)–2.26 (9) | 4.817 |
| Al1 | 5 | 1.78 (5)–2.15 (7) | 2.273 |
| Al2 | 6 | 1.71 (5)–2.13 (5) | 2.687 |
| Al3 | 4 | 1.63 (5)–1.74 (5) | 3.275 |
| Al4 | 6 | 1.60 (5)–2.13 (5) | 3.173 |
| Al5 | 6 | 1.58 (5)–2.23 (5) | 2.860 |
| Al6 | 6 | 1.76 (6)–2.25 (6) | 2.524 |
| Al7 | 4 | 1.73 (5)–1.82 (5) | 2.594 |
| Al8 | 4 | 1.74 (6)–1.78 (5) | 2.789 |
| Al9 | 5 | 1.77 (5)–2.15 (6) | 2.383 |
| Al10 | 6 | 1.79 (5)–2.10 (5) | 2.691 |
| Al11 | 6 | 1.78 (5)–2.13 (5) | 2.846 |
| Al12 | 4 | 1.6 (1)–1.75 (6) | 3.201 |
| Al13 | 5 | 1.67 (5)–2.17 (5) | 2.374 |
| Al14 | 5 | 1.52 (4)–2.18 (5) | 2.834 |
| Al15 | 4 | 1.71 (7)–1.96 (6) | 2.440 |

index (g.i.i.; Salinas-Sanchez *et al.*, 1992) of 0.26 valence units (v.u.). The largest deviation is −0.55 v.u. for Al7, which is comparable to isostructural $SrAl_8Ti_3O_{19}$, where the g.i.i. is 0.22 v.u. and the largest discrepancy of −0.47 v.u. on Al3. (Complete bond-valence sum calculations for $SrAl_8Ti_3O_{19}$ can be found in the supplementary material – Tables S1 and S2.) These acceptable deviations from AV can be attributed to intrinsic strains present in complex ternary oxides, or to the less accurate determination of O-atom positions by X-ray diffraction compared with La, Ti and Al, and consequently the $M$—O distances are less accurate. On the other hand, the deviations of BVS from AV for $La_3Ti_5Al_{15}O_{37}$ are significantly

**Table 6**
Bond-valence sums (BVS) for selected oxygen ions that deviate the most from their expected atomic valences, together with O—Ti/Al and O—La distance ranges in $La_3Ti_5Al_{15}O_{37}$ (CN = coordination number).

| Oxygen | CN | Distance ranges O—Ti/Al (Å) | Distance ranges O—La (Å) | BVS |
|---|---|---|---|---|
| O3 | 6 | 1.67 (4)–2.05 (9) | – | −4.393 |
| O1 | 4 | 1.60 (5)–1.96 (6) | – | −3.921 |
| O20 | 4 | 1.73 (8)–2.08 (5) | 2.23 (4)–2.65 (4) | −2.693 |
| O6 | 5 | 1.71 (6)–2.26 (7) | 2.84 (4) | −2.634 |
| O7 | 4 | 1.58 (5)–2.13 (5) | – | −2.600 |
| O25 | 3 | 1.71 (7)–2.10 (5) | 2.58 (3) | −1.380 |
| O2 | 4 | 1.72 (5)–2.36 (5) | 2.78 (4) | −1.366 |
| O17 | 3 | 1.77 (5)–1.92 (5) | 2.75 (4) | −1.322 |
| O10 | 5 | 2.22 (7)–2.24 (7) | 2.71 (5)–2.94 (4) | −1.134 |
| O23 | 2 | 1.81 (5)–1.98 (5) | – | −0.984 |

larger (Tables 5 and 6), which is also reflected in a very high g.i.i. of 0.64 v.u. Several atoms have unacceptably large deviations, *e.g.* Ti1, O1, O3 and O23 with discrepancies of +1.47, −1.92, −2.39 and +1.02 v.u. from nominal values. The O3 atom with three $Ti^{+4}$ and three $Al^{+3}$ cations in its first coordination sphere has an AV of −4.39 v.u. On the other hand, the O23 atom does not have enough cations in its neighborhood (only two $Al^{+3}$), resulting in an AV of only −0.98 v.u. To conclude, BVS calculations are physically unacceptable for $La_3Ti_5Al_{15}O_{37}$.

**3.3.4. The refinement procedure**. Morris *et al.* (1994) report that soft constraints were needed to prevent chemically unreasonable metal–metal bond distances in $La_3Ti_5Al_{15}O_{37}$, but these constraints were omitted in the final refinement cycles. On the other hand, no restraints and/or constraints were necessary during the structure refinement of $LaTi_2Al_9O_{19}$ to arrive at a chemically and physically reasonable outcome. It is concluded that $La_3Ti_5Al_{15}O_{37}$ does not exist and material studied by Morris *et al.* (1994) was $LaTi_2Al_9O_{19}$. Additionally, $LaTi_2Al_9O_{19}$ is less complex with a significantly smaller number of atoms in its asymmetric unit (31 *versus* 60) and enables us to arrive at an equivalent fit to the data.

## 4. Conclusion

$LaTi_2Al_9O_{19}$ was found by Rietveld analysis of conventional X-ray powder diffraction data to be isostructural with $SrAl_8Ti_3O_{19}$. The structure consists of network of $AlO_6$ and $TiO_6$ octahedra linked by $AlO_4$ tetrahedra and 12-fold-coordinated $La^{3+}$ ions. The bond-valence sum calculations confirm that the proposed structure complies with the rules of crystal chemistry, unlike the alternate description as $La_3Ti_5Al_{15}O_{37}$, which has an identical powder diffraction pattern and was synthesized as for $LaTi_2Al_9O_{19}$. On the basis of given arguments, we can conclude that $La_3Ti_5Al_{15}O_{37}$ does not exist and material studied by Morris *et al.* (1994) was $LaTi_2Al_9O_{19}$.

Financial support of the Ministry of Higher Education, Science and Technology of the Republic of Slovenia is gratefully acknowledged (grants P2-0091, P1-0175 and MR-29397).

## References


Ali, R., Izumi, F. & Yashima, M. (2006). *J. Am. Ceram. Soc.* **89**, 3805–3811.

Brown, I. D. (1992). *Z. Kristallogr.* **199**, 255–272.

Coelho, A. A. (2007). *TOPAS-Academic*, Version 4.1. Coelho Software, Brisbane, Australia.

Dowty, E. (2005). *ATOMS*, Version 6.2. Shape Software, Kingsport, USA.

Herbert, J. M. (1985). *Ceramic Dielectrics and Capacitors, Electrocomponent Science Monographs*, Vol. 6. New York: Gordon and Breach Science Publishers.

International Centre for Diffraction Data (2009*a*). *PDF*-2, Release 1995. Newtown Square, PA, USA.

International Centre for Diffraction Data (2009*b*). *PDF*-2, Release 2009. Newtown Square, PA, USA.

Kuang, X., Allix, M. M. B., Claridge, J. B., Niu, H. J., Rosseinsky, M. J., Ibberson, R. M. & Iddles, D. M. (2006). *J. Mater. Chem.* **16**, 1038–1045.

Morgan, P. E. D. (1984). *Mater. Res. Bull.* **19**, 369–376.

Morris, R. E., Owen, J. J., Stalick, J. K. & Cheetham, A. K. (1994). *J. Solid State Chem.* **111**, 52–57.

Salinas-Sanchez, A., Garcia-Muñoz, J. L., Rodriguez-Carvajal, J., Saez-Puche, R. & Martinez, J. L. (1992). *J. Solid State Chem.* **100**, 201–211.

Škapin, S., Kolar, D. & Suvorov, D. (1993). *J. Am. Ceram. Soc.* **76**, 2359–2362.

Slater, P. R. & Irvine, J. T. S. (1999). *J. Solid State Chem.* **146**, 437–438.

Strunk, M. & Mueller-Buschbaum, H. (1993). *J. Alloys Compd*, **198**, 101–104.

Suvorov, D., Valant, M., Škapin, S. & Kolar, D. (1998). *J. Mater. Sci.* **33**, 85–89.

Thompson, P., Cox, D. E. & Hastings, J. B. (1987). *J. Appl. Cryst.* **20**, 79–83.

Yoshioka, H. (1994). *Kidorui*, **24**, 124–125.

Zhang, Q. & McGinn, P. J. (2006). *J. Am. Ceram. Soc.* **89**, 1687–1693.